

The GUSBAD Catalog of Gamma-Ray Bursts

Maarten Schmidt

California Institute of Technology, Pasadena, CA 91125

ABSTRACT

The GUSBAD catalog of gamma-ray bursts (GRBs) is based on archival BATSE DISCLA data covering the full 9.1 years of the Compton Gamma Ray Observatory mission. The catalog contains 2204 GRBs, including 589 bursts not listed in the Current BATSE Burst Catalog. The GUSBAD catalog is uniform in the sense that the detection criteria are the same throughout and that the properties given in the catalog are available for every burst. The detection and the derivation of the properties of the GRBs were carried out automatically. This makes the GUSBAD catalog especially suitable for statistical work and simulations, such as used in the derivation of V/V_{\max} . We briefly touch upon a potential problem in defining a GRB duration that is physically meaningful.

Subject headings: cosmology: observations — gamma rays: bursts

1. Introduction

The Burst and Transient Source Experiment (BATSE) (Fishman et al. 1989) on board the *Compton Gamma Ray Observatory (CGRO)* has been very successful in detecting gamma-ray bursts (GRBs). The data have been published in a succession of catalogs, the most recent of which is the Current BATSE Burst Catalog¹ ('the BATSE catalog'). The 2702 GRBs in the BATSE catalog are the result of the full mission of *CGRO* from 1991 April 19 to 2000 May 26.

Burst detections are based on counts recorded by eight Large Area Detectors (LADs) located at the corners of the spacecraft (Fishman et al. 1989). Counts are collected in four energy channels (20 – 50, 50 – 100, 100 – 300 and > 300 keV) on time scales of 64, 256, and 1024 ms. All GRBs in the BATSE catalog are based on an on-board trigger mechanism, which acted when certain conditions were fulfilled. Usually these required that the LAD

¹Available at <http://www.batse.msfc.nasa.gov/batse/grb/>.

counts in the energy range 50 – 300 keV exceeded the background by at least 5.5σ on a time scale of 64, 256 or 1024 ms in at least two of the eight BATSE detectors. The background for each detector was averaged over 17.408 s, immediately preceding the burst and was recomputed every 17.408 s (Fishman et al. 1989). The trigger mechanism was disabled for up to 90 minutes following a burst detection to allow telemetering burst data to the ground. It also was disabled during passage through regions with a high density of atmospheric particle precipitation events (Fishman et al. 1994). The BATSE catalog gives for each GRB the time of detection, celestial coordinates, maximum and minimum count rates, peak flux, fluence and durations whenever available.

For statistical studies the BATSE catalog has some serious drawbacks. The maximum and minimum count rates, needed to derive V/V_{\max} , are available for only $\sim 49\%$ of the 2702 GRBs. Also, the catalog is not uniform in the sense that the trigger criteria were changed many times through the mission; the standard parameters mentioned above were in effect for $\sim 55\%$ of the mission duration.

A catalog of GRBs without these drawbacks can be constructed from archival data produced by BATSE. For this purpose we have used the DISCLA data which provide a continuous record of the LAD counts in the four energy channels on a time scale of 1024 ms for each of the eight BATSE detectors. These data allow the *a posteriori* detection of GRBs with a software trigger in a manner similar to that executed by the on-board trigger mechanism. The availability of only the 1024 ms timescale means that the search will be essentially limited to bursts with a duration of more than 1 – 2 s. There are distinct advantages in using a software trigger on the continuous data stream. One can experiment with the derivation of the background or can repeat the search for bursts with different detection criteria. We have carried out such a search resulting in the GUSBAD catalog (Gamma-ray bursts Uniformly Selected from BATSE Archival Data) (Schmidt 2003)² The GUSBAD catalog supercedes earlier work on DISCLA data reported in Schmidt (1999a,b).

In order to allow simulations, such as used in the derivation of V/V_{\max} , we were guided by the following precepts in the search for GRBs. The detection and the derivation of burst events should be carried out automatically. We search for bursts only at times when all properties of a burst event can be derived. Also, we treat strong bursts no differently from weak bursts. We worked independently from other catalogs, such as those of Kommers et al. (1997) and Stern et al. (2001), which were under development while this work was in progress; however, in the classification procedure (see Sec. 3) we did use the listing of any GUSBAD burst event in the BATSE catalog as confirmation that the event was a cosmic

²Available at <http://www.astro.caltech.edu/~mxs/grb/GUSBAD/>.

GRB.

We describe in Sec. 2 the treatment of the DISCLA data, the definition of the trigger mechanism and the derivation of the celestial coordinates of burst events. In Sec. 3 we discuss the classification of the triggers required to separate the cosmic GRBs from other types of events. Sec. 4 covers the derivation of exposure and effective limiting peak flux and Sec. 5 the simulation producing the Euclidean value of V/V_{\max} . The GUSBAD catalog is described in Sec. 6. The discussion in Sec. 7 includes comments on the problem of defining a robust GRB duration.

2. Burst Events from DISCLA Data

2.1. DISCLA Data

DISCLA data provide every 1024 ms counts in the four energy channels for each of the eight BATSE LAD detectors (Fishman et al. 1989) and every 2048 ms information about the orientation and geocentric coordinates of *CGRO*. We used for the time period TJD 8365 – 10528 a tape copy of DISCLA data made available by T. Prince, and for TJD 10529 – 11690 data obtained from the High Energy Astrophysics Science Archive Research Center (HEASARC).

2.2. Trigger Definition

For the detection of a burst we use a software trigger requiring that the counts in the 50 – 300 keV energy range exceed the background by at least $5.0\sigma_B$ in two or more of the eight BATSE detectors, where σ_B is the standard deviation of the background counts. Let $C_d(k)$ be the measured number of counts in 1024 ms time bin k for detector d . To estimate the number of background counts $B_d(k)$, we average the counts in time bins $k - n_p - n_b, \dots, k - n_p - 1$ to produce B_{d1} , and in time bins $k + n_f + 1, \dots, k + n_f + n_b$ to get B_{d2} . We adopt $n_b = 17$ as was done for the on-board BATSE trigger. We also use $n_p = 20$ and $n_f = 225$ and derive $B_d(k)$ from a linear interpolation between B_{d1} and B_{d2} , see Figure 1. The signal-to-noise ratio of the excess counts is $S_d(k) = [C_d(k) - B_d(k)]/[B_d(k)]^{1/2}$; if it is larger than 5.0 in two detectors, we record the onset of a burst event in time bin k_{trig} .

The interval n_p between the first background interval and the test bin was introduced to allow detection of slowly rising bursts which may have escaped detection with the BATSE trigger (Higdon & Lingenfelter 1996). In setting the n_f value, we essentially assume that

the duration of the GRB is less than 230.4 s. The effect of some burst signal in the second background interval usually will be minor given its low weight in the interpolated background. Some very long bursts required special treatment, see Sec. 3.

To make sure that all properties can be derived for each recorded burst, we limit the search to bins in which the counts are recorded and uncontaminated from $k - n_f - n_b$ to $k + n_p + n_b$. Interruptions were caused by high voltage switch-off for the South Atlantic Anomaly; poor data were identified by checking for instances where several detectors recorded a zero or constant count. We also excluded appropriate time intervals around checksum errors reported in DISCLA data, which turned out to mimick short bursts. Ultimately, we identified a total of 199,964 time windows of different lengths which were excluded from the search.

In an early search for GRBs based on the period TJD 8365-10528, we found strong concentrations of triggered events recorded in geographical areas over W. Australia, Texas and an area bordering the South Atlantic Anomaly (Schmidt 1999a). To avoid searching for cosmic GRBs in such a high density of non-cosmic triggers, we established geographical exclusion regions around the areas of highest density. This reduced the total number of triggers by $\sim 40\%$.

2.3. Celestial Coordinates

The burst events detected are composed of many different sources besides cosmic GRBs, see Sec. 3. In the classification procedure required to find the nature of the events, celestial coordinates play an important role. We discuss here the derivation of positions on the assumption that the burst event is a point source. We start by setting up a grid of $\sim 40,000$ positions, separated by $\sim 1^\circ$ in an equatorial coordinate system anchored on the satellite. Using the BATSE DRM generator code supplied by J. Brainerd, we derive at each of these positions the effective cross-section for each detector, ignoring the scattered radiation part of the DRM. We use a Band spectrum (Band et al. 1993) with $\alpha = -1.0$, $\beta = -2.0$ and $E_0 = 200$ keV. The position of a burst event is derived by finding in which of the 40,000 grid positions the observed counts produce the largest amplitude for the burst. Our procedure involves the use of all eight detectors. We determine the positions from each time bin in which the burst is exceeding the minimum detectable flux. The ultimate position is derived from the sum of the counts in all the time bins with reasonably concordant positions; this part does include an iteration which accounts for the radiation off the Earth's atmosphere and the satellite. The specific steps are given below.

Based on the background (by linear interpolation between B_{d1} and B_{d2}) used at the time of trigger, derive the net burst counts in each detector in 225 time bins starting with k_{trig} . For each of the 40,000 grid positions, carry out a least-squares solution to derive a photon flux from the net counts in the eight detectors; the largest derived flux sets the position of the trigger event. Use this flux f_{trig} and the signal-to-noise ratio in the second brightest illuminated detector at trigger to derive the minimum detectable flux f_{min} corresponding to a signal-to-noise ratio of 5.0. Derive the positions independently for each of the 225 time bins in which the flux $f > f_{\text{min}}$. Starting at k_{trig} successively monitor the average position and reject positions that deviate by more than 20° from the average. For the bins with accepted positions, sum the net burst counts accumulated during the burst. Using the summed net counts, derive the satellite-anchored celestial coordinates. Correct the net counts for scattered radiation, re-derive the celestial coordinates as before and iterate. From the final position so derived and the positions obtained from each contributing time bin, derive the standard deviation of one position, and the apparent angular rate of motion across the sky.

3. Classification of Events

The search for burst events covered a total of around 250 million time bins, each of which was tested for the presence of a burst. Using the procedures described above, we found 6236 burst events. Figure 2 shows the equatorial coordinates of all the triggers. The figure shows four types of events. Most prominent are CygX-1 and GRO J0422+32 (= Nova Persei 1992) in the N. hemisphere. The sun exhibits itself through solar flares along the ecliptic. A fourth component appears to be more or less isotropic.

The outburst of GRO J0422+32 affords an opportunity to evaluate the accuracy of our burst positions. From TJD $\sim 8840 - 8900$ the X-ray nova was active, producing a total of ~ 400 bursts. At the peak of its activity, we recorded 165 burst events in four days, from TJD 8841-44. Three of these events were located at distances of 58° , 63° and 152° , respectively, from the nova. The other 162 were all within 20° and clearly associated with the nova, see Figure 3. The standard deviation from the mean is $\pm 7.5^\circ$. The average photon flux of these events was $\sim 0.26 \text{ ph cm}^{-2} \text{ s}^{-1}$, i.e. similar to the weakest GRBs in the GUSBAD catalog.

Plots of the rate of burst events versus time for positions close to the sun, CygX-1 and GRO J0422+32 show well defined periods of activity. We eliminated as GRB candidates all events within 17° of these sources while they were active. Plots of the hardness ratio $\text{ch } 1 / (\text{ch } 2 + \text{ch } 3)$ versus either angular distance to the sun or altitude of the sun showed that there were still a number of soft events associated with the sun. A correlation of triggers with known solar flares also produced some positive results. As for CygX-1 during its less active

periods, a number of positive jumps in the counts were seen corresponding to its rising above the horizon, and many cases were found where the counts showed fast oscillations apparently associated with CygX-1 based on the positions. Eventually, we eliminated as GRB candidates over 1500 triggers which were solar flares or close to the sun, upwards of 760 triggers close to or associated with CygX-1 and over 400 triggers near GRO J0422+32.

At this stage we correlated all remaining events with the BATSE catalog. All events with onsets within $(-15, +30)$ s from that of a BATSE GRB and a position difference less than 30° were considered confirmed as cosmic GRBs. The decision whether this also applied to the triggers with larger differences in trigger time (up to 230 s) or position was mostly based on the time profile. This exercise showed that 1615 burst events were present in the BATSE catalog and therefore confirmed as GRBs.

For the ~ 2100 remaining triggers, we inspected the time profiles in each of the eight detectors over 700 s around the trigger time, in some cases in the two brightest illuminated detectors over an interval of 12000 s. At this stage, we were guided by descriptions of magnetospheric events (Fishman et al. 1992; Horack et al. 1992) which caused many of the remaining bursts. In evaluating each event, besides the time profile we also paid attention to the values of χ^2 and the rms deviation of the positions for each time bin (see Sec. 2.3), the apparent angular motion of the burst event (which for a GRB should be zero), and the altitude of the event (the horizon being at -18°). This exercise resulted in the rejection of around ~ 1300 triggers.

In addition to six detections of SGR 1806 – 20, we have some 50 triggers from a variable near 285 + 10 from TJD 10959 – 11145 and around 40 near 250 – 55 from TJD 10981 – 11026. We also checked for the presence of variables based on a list provided by B. Harmon, but found no further ones.

Based on a review of the surviving GRB candidate triggers, 19 GRBs were found to have been detected twice and one GRB three times. Also, in six cases the derivation of positions was affected by the occurrence of a second burst, by saturation or by unexpected bad data. These cases were all handled individually. We finally ended up with 589 GRBs that are not listed in the BATSE catalog. Together with the 1615 GRBs that are in the BATSE catalog, we have a total of 2204 GRBs in the GUSBAD catalog.

4. Exposure and Limiting Flux

We investigate the total exposure and limiting photon flux of the GUSBAD catalog by setting up a $10 \times 10^\circ$ grid of 412 sky positions. Every 100 s during the entire mission, we used

our detection algorithm to derive the background in the second brightest illuminated detector at each of the 412 positions and with the DRM generator (ignoring scattered radiation) obtained the limiting photon flux corresponding to a signal-to-noise ratio of 5.0. The effect of scattered radiation off the Earth atmosphere and the space craft was similarly explored once every ten days during the mission. We averaged the results over all sky positions and accounted for the rejection of triggers near the sun, CygX-1 and GRO J0422+32 when active, as well as Earth blockage. The total exposure time was 1.0052×10^8 s or 3.185 years. It corresponds to the total time during which the GRB search was effectively carried out over the entire celestial sphere. Figure 4 shows the distribution of exposure with limiting photon flux, both with and without the effect of scattered radiation.

For statistical work such as deriving the V/V_{\max} value, it may be sufficient to use an effective photon limit that yields the same number of sources over the total exposure time as does a proper evaluation using the distribution of photon limits. For values of the integral source count slope in the range -0.5 to -1.0 applicable to the faintest GRBs in the GUSBAD catalog, the effective limiting photon flux is $0.25 \text{ ph cm}^{-2} \text{ s}^{-1}$. If this limit is used for statistical purposes, all GRBs listed in the catalog should be included.

The annual rate of GRBs averaged over the full mission but corrected for Earth occultation is $2204/3.185 = 692 \text{ y}^{-1}$. The integral GRB source counts $N(> P)$ as a function of peak flux P are shown in Figure 5. At the bright end the logarithmic slope is close to the value $-3/2$ consistent with a uniform space distribution in Euclidean space. The effect of the decrease of exposure time for $P < 0.3 \text{ ph cm}^{-2} \text{ s}^{-1}$ is clearly seen.

5. Deriving V/V_{\max}

For extragalactic objects, the Euclidean value of $\langle V/V_{\max} \rangle$ is a cosmological distance indicator (Schmidt 2001). The value of V/V_{\max} for a GRB is usually derived from the peak burst count rate C_{\max} and the limiting detection rate C_{\min} as $(C_{\max}/C_{\min})^{-3/2}$. This is not strictly correct as we shall see.

We derive the value of V/V_{\max} of an individual GRB by a simulation. The simulation is best visualized as an exercise in which the distance of the burst is incrementally increased in Euclidean space until it becomes undetectable. The full time profile of the burst is reduced by a factor corresponding to the increased distance and then added back to the original interpolated background (see Fig. 1). The detection algorithm is employed to search for the reduced burst. If it is detected, the process - including the full search - is repeated until the burst is not detected anymore. If the burst is lost when the distance has been

increased by a factor f then $V/V_{\max} = f^{-3}$. The 2204 GRBs in the GUSBAD catalog have $\langle V/V_{\max} \rangle = 0.346 \pm 0.006$.

In the process of analyzing the reduced burst profiles, the trigger may occur at later times depending on the detailed profile. (If this causes the second background stretch to suffer from contaminated or missing data, it is kept at its location during the original detection.) If so, the two background stretches defined in Fig. 1 move forward and the first background stretch may contain burst signal. This reduces the amplitude of the reduced burst and increases the background. Hence V/V_{\max} derived from the simulation is larger than $(C_{\max}/C_{\min})^{-3/2}$. This is confirmed in the GUSBAD catalog which yields $\langle (C_{\max}/C_{\min})^{-3/2} \rangle = 0.335$. In the BATSE catalog, only 884 of the 1144 GRBs with $C_{\max}/C_{\min} \geq 1.0$ on a timescale of 1024 ms can be used for a comparison: the others fall at times when the on-board trigger used parameters other than the standard mentioned in Sec. 1. They yield $\langle (C_{\max}/C_{\min})^{-3/2} \rangle = 0.311 \pm 0.009$.

6. The GUSBAD Catalog

The GUSBAD catalog is available on the World Wide Web (Schmidt 2003)³. The designation of GRBs in the catalog is GUSBAD YYMMDD.ddd where Y, M, D are integral year, month and day numbers, respectively, and .ddd is the truncated fraction of the day. The strong source GUSBAD 950203.097 not listed in the BATSE catalog is illustrated in Figure 6. The main properties listed in the catalog are as follows. Besides equatorial (RA, dec) coordinates two other types of positions are provided for the time of detection, namely azimuth and altitude, and in an equatorial system anchored on BATSE. Four time bins are listed, viz., k_{trig} to mark the detection (see Sec. 2.2), k_{top} for the peak of the time profile, k_{last} for the last detection above the photon flux limit, and k_{far} for the final detection in the simulation for V/V_{\max} discussed in Sec. 5. Photon peak flux, fluence and V/V_{\max} are listed, as well as the brightest and second brightest illuminated detectors. The hardness ratios $\text{ch}(x)/(\text{ch } 2 + \text{ch } 3)$ are given for $x = 1 - 4$ as well as the spectral index derived from the counts in channels 2 and 3.

³Available at <http://www.astro.caltech.edu/~mxs/grb/GUSBAD/>.

7. Discussion

The GUSBAD catalog lists 589 GRBs that are not in the BATSE catalog. How many GRBs in the BATSE catalog are missing from the GUSBAD catalog? For this purpose, we have to limit the comparison to the 1144 GRBs in the BATSE catalog that have $C_{\max}/C_{\min} \geq 1.0$ on a timescale of 1024 ms. Among these, we find that the GUSBAD catalog is missing 156 BATSE sources. There are several reasons why the catalogs have different contents. One reason is that the backgrounds used in the two catalogs are semi-independent. The background used for the BATSE catalog is covering a time stretch of 17.408 s preceding the burst detection by a time interval anywhere from 0.0 to 17.344 s. The first background stretch used in the GUSBAD detections also covers 17.408 s but precedes the burst detection by 20.0 s. Therefore, depending on circumstances, the two backgrounds range from independent to mostly overlapping. It is useful to remember that for independent backgrounds, the probability that a source in one survey is detected in the other is $\sim 50\%$ if the source is at the detection limit. Another source of difference in catalog content has to do with the search procedure. For the GUSBAD catalog, we avoided high densities of triggers related to geographical location, proximity to active sources (sun, CygX-1, etc), and poor data. The on-board trigger for the BATSE sources at the 1024 ms time scale was disabled over regions of high magnetospheric activity, and following a burst event to allow transmission of data to the ground.

The positions of GRBs in the GUSBAD catalog were derived from an algorithm employing counts from all eight BATSE detectors. The internal mean errors of the positions are $\pm 7.5^\circ$ (see Sec. 3), based on bursts of GRO J0422+32, which were typically near our detection limit. For 439 weak GRBs in the BATSE catalog with $1.0 < C_{\max}/C_{\min} < 2.0$ the r.m.s. value of the listed location errors is $\pm 6.8^\circ$. A comparison of positions of GRBs common to the two catalogs shows a r.m.s. dispersion of the difference of $\pm 9.8^\circ$, but the interpretation of this value is difficult, since the GUSBAD and BATSE positions are not independent. The positions given in the BATSE catalog were based on the six (originally four) detectors whose normals are closest to the source position. The move from four to six detectors led to some changes in position as large as $50^\circ - 100^\circ$ (Meegan et al. 1996).

We originally defined in this work the duration of a GRB as the total time span from trigger to last observation above the detection limit, so $T = 1.024(k_{\text{last}} - k_{\text{trig}} + 1)$ s. It is useful in outlining the time interval in which information about positions, spectral properties, etc. can be obtained. As discussed in Sec. 5, when we reduce the burst amplitude in the simulation leading to V/V_{\max} , the detection time may move forward, depending on the time profile of the burst. Similarly, the end of the reduced burst, may happen earlier and earlier. So T will decrease as the burst amplitude is reduced. We find, in fact, that most bursts have

at the simulated limit of detection a duration of one bin of 1.024 s only. This is to be expected: if there were two bins left above the detection limit, the amplitude could be reduced further resulting in only one bin. The variation of T with simulated burst amplitude is so strong that it makes it useless as an indicator of the physical duration of a GRB. This phenomenon is similar to the fluence duration bias in the BATSE catalog discussed by Hakkila et al. (2000). The question as to whether there is any definition of GRB duration that is robust and physically meaningful is beyond the scope of this article.

Following the declination of a grant proposal to the National Aeronautics and Space Administration (NASA) in 1994, this work was carried out and completed without benefit of funds. This research made use of data obtained from HEASARC, provided by NASA's Goddard Space Flight Center. It is a pleasure to thank J. Bonnell, J. Brainerd, D. Chakrabarty, V. Connaughton, M. Finger, G. Fishman, J. Gunn, A. Harmon, J. Higdon, J. Horack, M. McCollough, C. Meegan, G. Pendleton, T. Prince, C. Shrader, B. Vaughan and K. Watanabe for assistance or information supplied during this project.

REFERENCES

- Band D. L. et al. 1993, *ApJ*, 413, 281
- Fishman, G. J. et al. 1989, *GRO Science Workshop Proc.*, W. N. Johnson, Greenbelt: NASA, 2-39
- Fishman, G. J., Meegan, C. A., Wilson, R. B., Horack, J. M., Brock, M. N., Paciasas, W. S., Pendleton, G. N. & Kouveliotou, C. 1992, *AIP Conf. Proc.* 265, W. S. Paciasas & G. J. Fishman, New York: AIP, 13
- Fishman, G. J. et al. 1994, *ApJS*, 92, 229
- Hakkila, J., Meegan, C. A., Pendleton, G. N., Mallozzi, R. S., Haglin, D. J. & Roiger, R. J. 2000, *AIP Conf. Proc.* 526, *Gamma-Ray Bursts*, R. M. Kippen, R. S. Mallozzi & G. J. Fishman, New York: AIP, 48
- Higdon, J. C. & Lingenfelter, R. E. 1996, *AIP Conf. Proc.* 384, *Gamma-Ray Bursts*, C. Kouveliotou, M. F. Briggs & G. J. Fishman, New York: AIP, 402
- Horack, J. M., Fishman, G. J., Meegan, C. A., Wilson, R. B. & Paciasas, W. S., 1992, *AIP Conf. Proc.* 265, W. S. Paciasas & G. J. Fishman, New York: AIP, 373
- Kommers, J. M., Lewin, W. H. G., Kouveliotou, C., van Paradijs, J., Pendleton, G. N., Meegan, C. A. & Fishman, G. J. 1997, *ApJ*, 491, 704
- Meegan, C. A. et al. 1996, *AIP Conf. Proc.* 384, *Gamma-Ray Bursts*, C. Kouveliotou, M. F. Briggs & G. J. Fishman, New York: AIP, 291
- Schmidt, M. 1999a, *A&AS*, 138, 409
- Schmidt, M. 1999b, *ApJ*, 523, L117
- Schmidt, M. 2001, *ApJ*, 552, 36
- Schmidt, M. 2003, *GUSBAD Catalog*
- Stern, B. E., Tikhomirova, Y., Kompaneets, D., Svensson, R. & Poutanen, J. 2001, *ApJ*, 563, 80

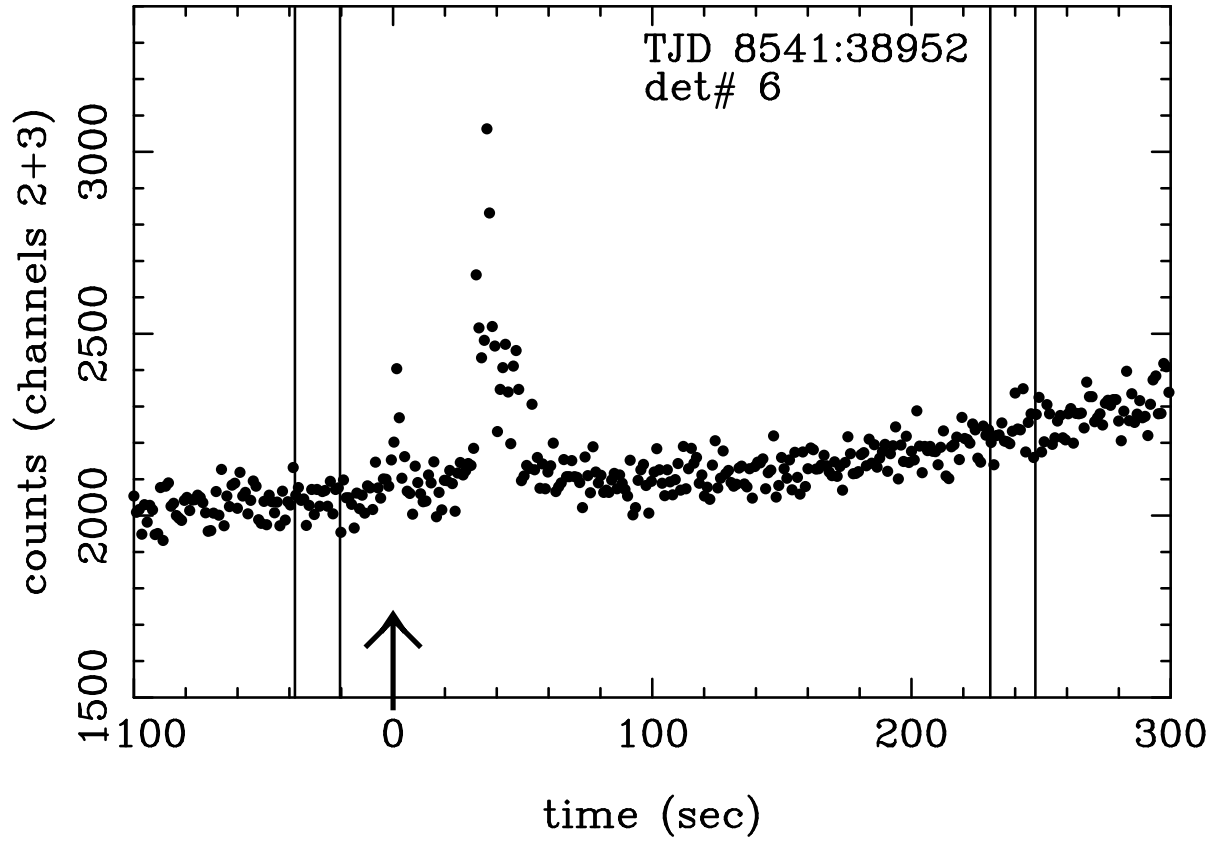


Fig. 1.— In testing for the presence of a burst at $t = 0.0$, the background is linearly interpolated between windows centered at -28.7 s and $+239.1$ s.

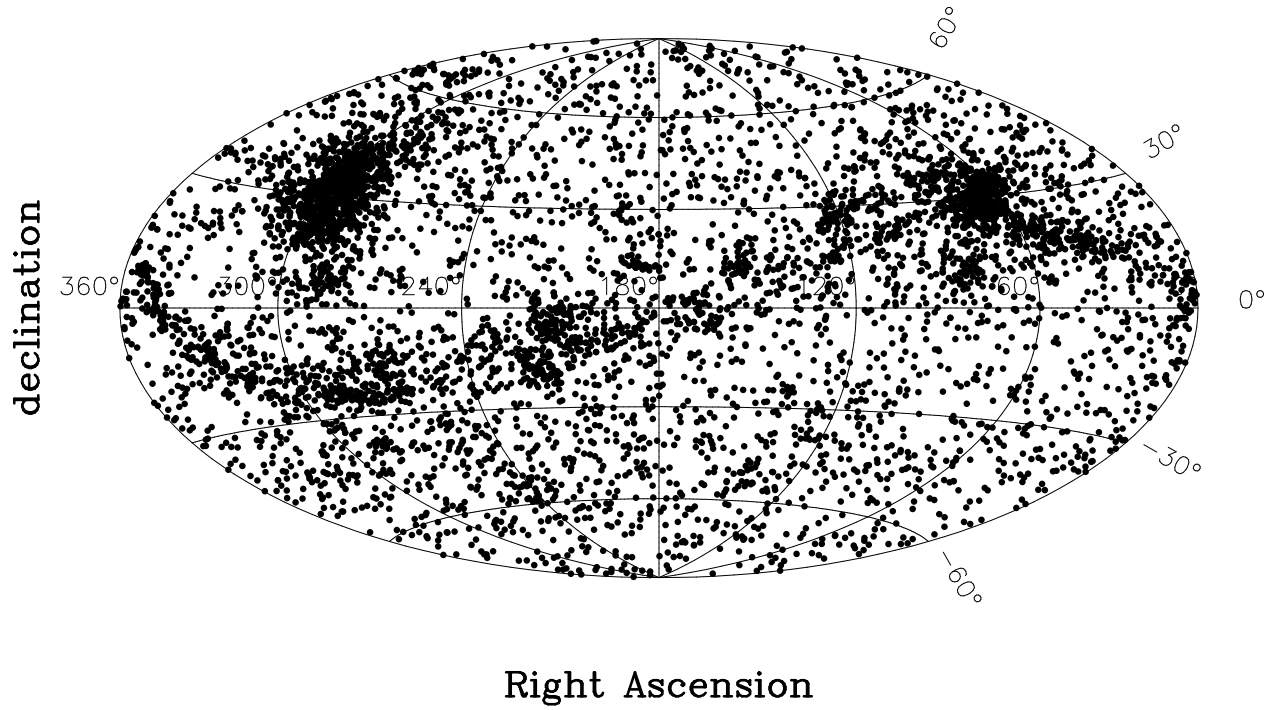


Fig. 2.— Equatorial coordinates of 6236 trigger events. In the N. hemisphere, CygX-1 and GRO J0422+32 are clearly seen. More than 1500 solar flares outline the ecliptic. The remaining triggers are mostly composed of magnetospheric events and cosmic GRBs.

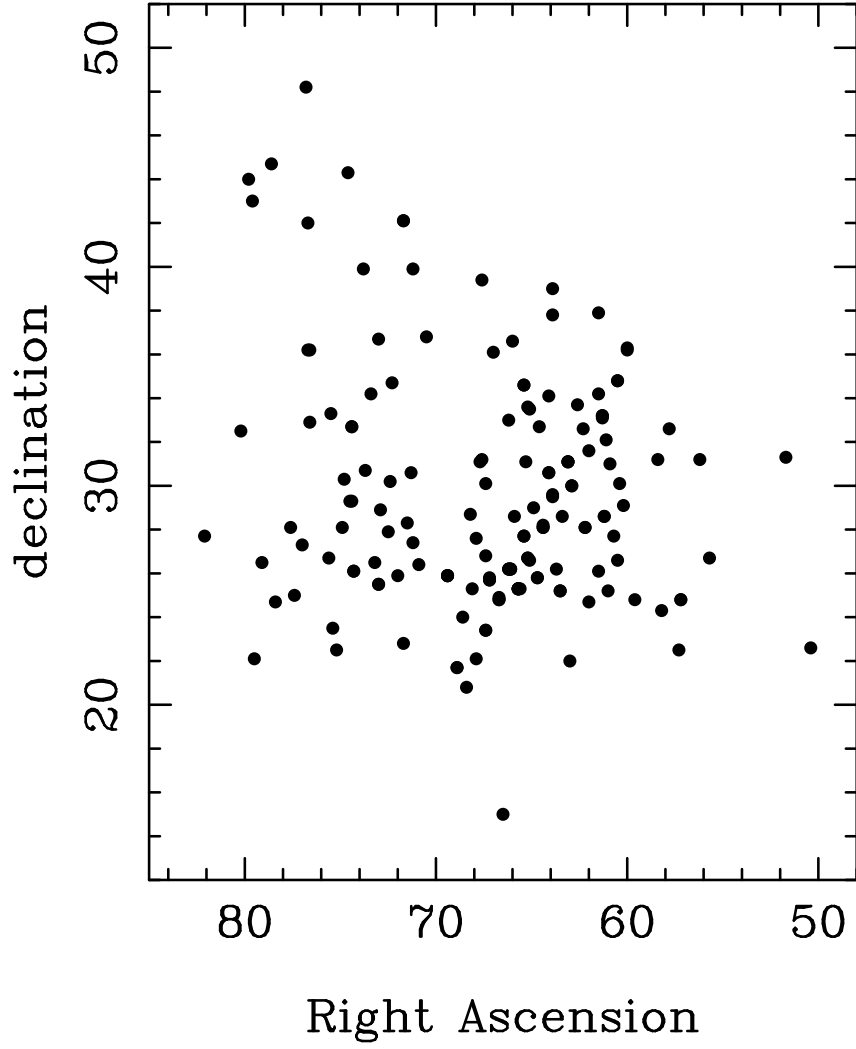


Fig. 3.— Equatorial coordinates for 162 triggers of GRO J0422+32.

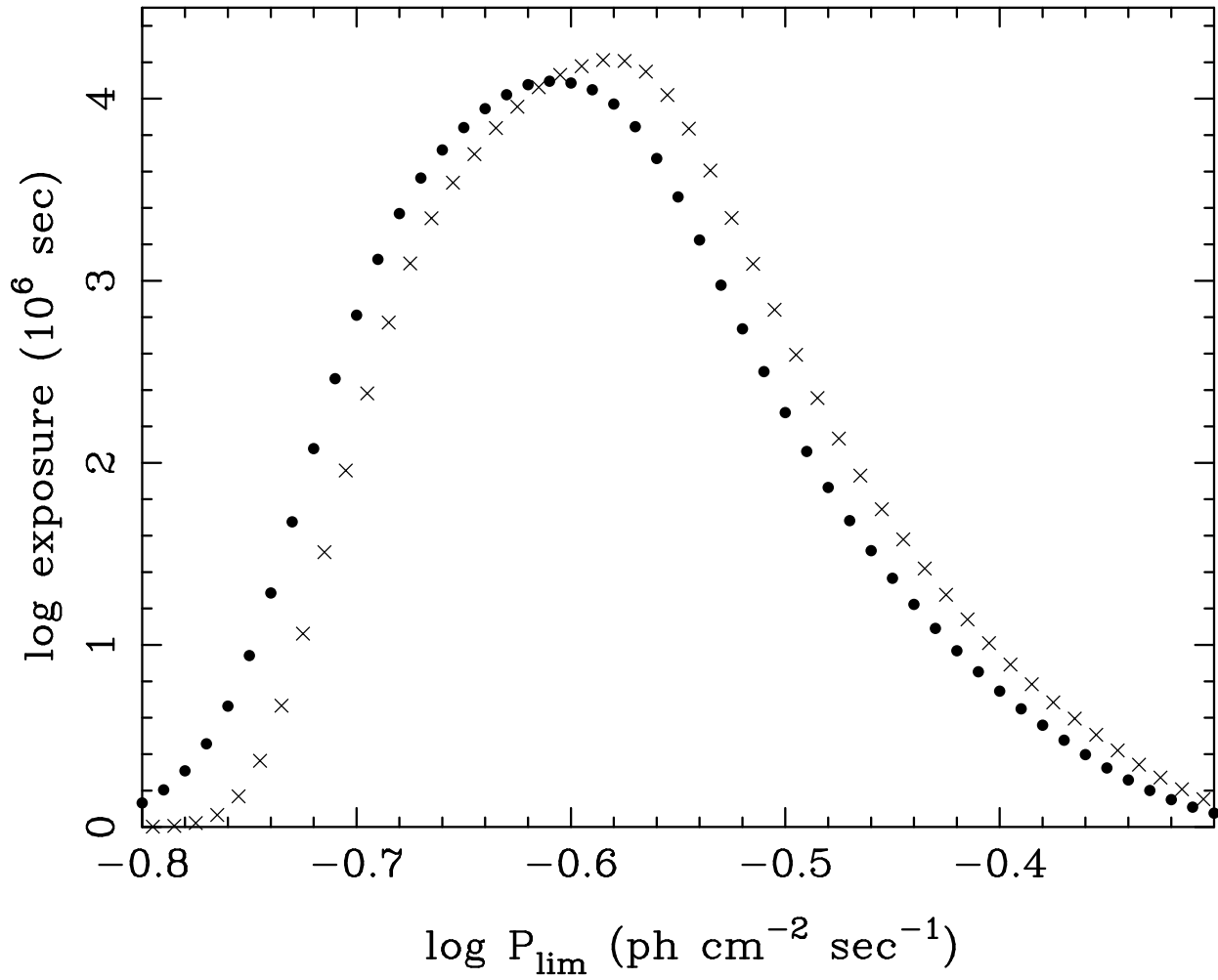


Fig. 4.— Exposure as a function of limiting peak flux P_{lim} . The crosses apply to direct radiation only; the dots include the effect of scattered radiation. The sum of the ordinates is the total exposure 1.0052×10^8 s.

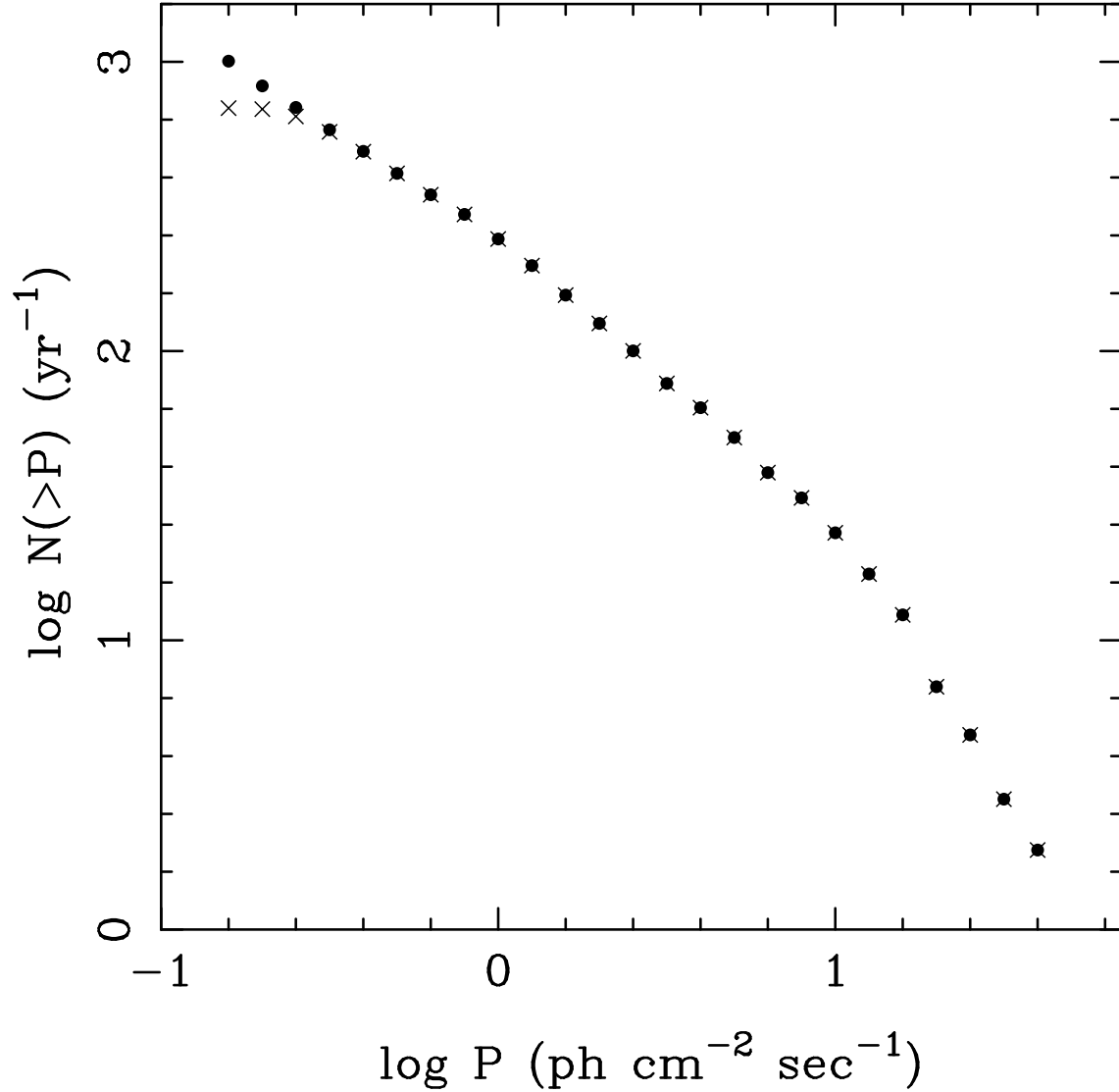


Fig. 5.— Integral GRB source counts $N(> P)$ as a function of peak flux P . Crosses are based on the raw source counts and the total exposure time of 3.185 y; the dots account for the variation of exposure time with P (see Fig. 4).

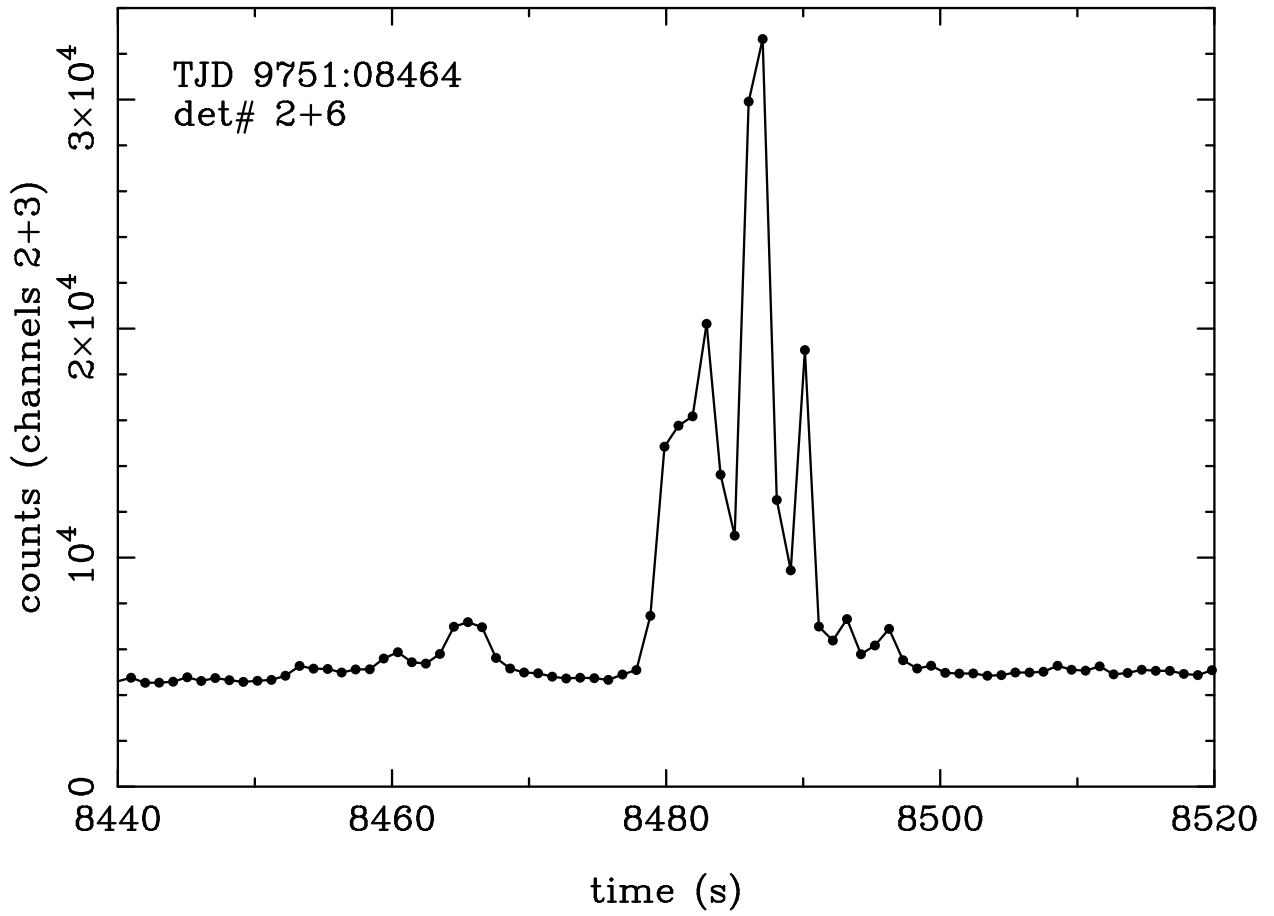


Fig. 6.— GUSBAD 950203.097 is the strongest GUSBAD GRB not listed in the BATSE catalog.